Molecular Dynamics Simulation of the Heterodimeric mGluR2/5HT$_{2A}$ Complex. An Atomistic Resolution Study of a Potential New Target in Psychiatric Conditions

Agostino Bruno,[†] Antonio Entrena Guadix,[‡] and Gabriele Costantino*,[†]

Dipartimento Farmaceutico, Via G. P. Usberti 27/A- Campus Universitario, Università degli Studi di Parma, 43124 Parma, Italy, and Departamento de Química Farmacéutica y Orgánica, Facultad de Farmacia, Universidad de Granada, Campus de Cartuja s/n, 18071 Granada, Spain

Received February 24, 2009

Homo- and heterodimerization is becoming an assessed concept in G-protein coupled receptor (GPCR) pharmacology, and the notion that GPCRs may dimerize or oligomerize is allowing for a reinterpretation of some inconsistencies or anomalies and is providing medicinal chemists with potentially relevant novel molecular targets for a variety of therapeutic conditions. Recently, it has been reported that two unrelated GPCRs, namely class C metabotropic glutamate receptor type-2 (mGluR2) and class A 5HT$_{2A}$ serotoninergic receptor, can heterodimerize at the transmembrane domain level. We performed a 40 ns molecular dynamics simulation of the mGluR2/5HT$_{2A}$ heterocomplex constructed around a TM4/TM5 interface and embedded in an explicit phospholipidic bilayer surrounded by water molecules. In a separate experiment, the monomeric 5HT$_{2A}$ receptor was simulated for additional 40 ns under the same conditions. The analysis and the comparison of the two simulations allowed us to clearly identify a cross-talk between the two protomers and to put forward an effect of the heterodimerization on the shape of the binding pocket of 5HT$_{2A}$. This result provides the first molecular explanation for the reported allosteric effect of mGluR2 on 5HT$_{2A}$-mediated response and suggests that the heterocomplex can be a more suitable target for in silico screening than the monomeric protomers.

INTRODUCTION

Homo- and heterodimerization of G-protein coupled receptors (GPCRs) is becoming an assessed concept, and the notion that GPCRs may dimerize or even oligomerize under physiological conditions is allowing for a reinterpretation of some inconsistencies and anomalous observations in GPCR pharmacology. Furthermore, GPCR dimers and oligomers are being perceived as molecularly different targets with respect to their monomeric protomers, thus suggesting an extending scope in their druggability.[1–3] Examples of homo- and heterodimers have been reported for family A GPCRs[4–6] and, as a particularly relevant case, for members of the family C of GPCRs, namely metabotropic glutamate receptors (mGluRs) and GABA$_B$ receptors, for which functional dimers have been early reported,[7,8] and for which the dimeric form is accepted to be the constitutive functional unit.[8–10] Recently, evidence for the heterodimerization between the subtype-2 of the mGluR family and the 5HT$_{2A}$ subtype of the seretoninergic family have also been reported,[11] thus indicating that dimerization can also occur among unrelated receptor subtypes. Furthermore, the existence of a functional dimer between mGluR2 and 5HT$_{2A}$ has been associated with important functional consequences related to the mechanism of action of antipsychotic drugs, for which both receptor subtypes are considered druggable targets.[12–14]

The notion that GPCR homo- and heterodimerization is a highly frequent phenomenon, with broad functional implication, allows for the reinterpretation of some unusual or anomalous observations made in the past years in the field of GPCR pharmacology and provides potentially exploitable new targets for a variety of therapeutic conditions.[11,15,16] In this context, several models of GPCRs have been previously proposed, facilitated by the resolution of the crystal structures of rhodopsin, and, more recently, β1 and β2-adrenergic and A$_{2A}$ adenosine receptors, and these models have been widely employed in drug discovery programs for virtual screening or structure-based ligand design.[17–20] Given the increasingly recognized functional importance of dimeric or oligomeric GPCR aggregates,[10,15,16,21,22] one can ask whether explicit models of homo- or heterodimers can better address issues related to ligand recognition or receptor activation. With the aim of shedding some light on this aspect, we decided to investigate the particularly interesting case of the heterodimer formed by the unrelated class C metabotropic glutamate receptor type 2 (mGluR2) and the class A serotoninergic receptor type 2A (5HT$_{2A}$).[11,23] The following are particularly relevant points: (i) this aggregate is made up of two unrelated protomers belonging to different classes of the superfamily of GPCRs; (ii) heterodimerization with mGluR2 increases the affinity of 5HT$_{2A}$ for a particular class of hallucinogen compounds (Chart 1), while activation of the glutamate component of the dimer by mGluR2 agonists suppresses the hallucinogen specific response, thus indicating the occurrence of an allosteric cross-talk between the two protomers; and (iii) the heterodimerization is selective, as the closely related mGluR3 subtype did not form functional dimers with 5HT$_{2A}$ under the same experimental conditions as mGluR2 did.[11]

* Corresponding author phone: +30 0525 905054; fax: +39 0525 905006; e-mail: gabriele.costantino@unipr.it.
[†] Università degli Studi di Parma.
[‡] Universidad de Granada.

10.1021/ci900067g CCC: $40.75
Published on Web 05/07/2009

Chart 1. Selected Examples of Hallucinogen and Nonhallucinogen Serotonin Agonists

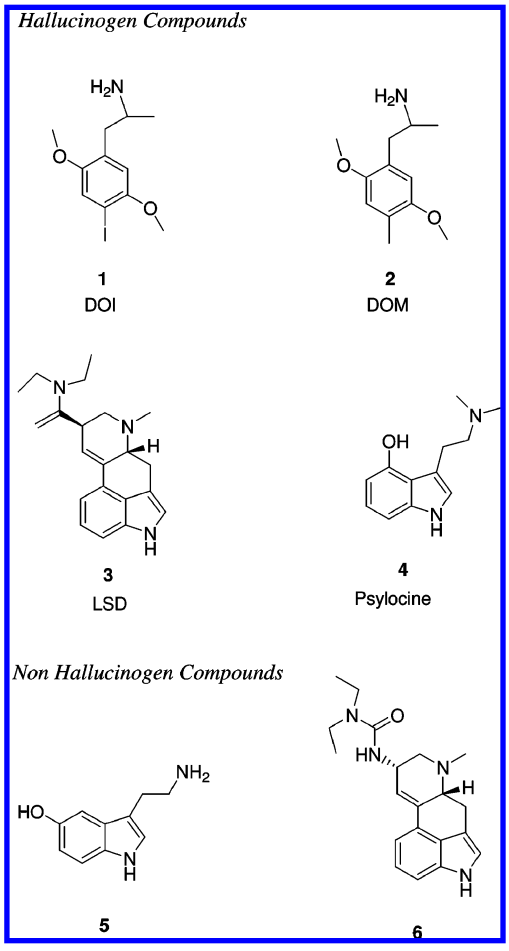

Taken together, this information suggests that heuristic constructs of the mGluR2/$5HT_{2A}$ dimer can have the potential for being better models than the corresponding monomeric models, either in terms of drug discovery efforts or in supporting experiments aimed at deciphering the molecular basis of receptor activation.

The problem of generating working models of homo- or heterodimeric GPCRs requires essentially (a) the correct definition of the dimerization interface and (b) the ability to detect allosteric cross-talk between the homo- or heteroprotomer through the interface. For the definition of the dimerization interface, several bioinformatics approaches have been proposed flanking experimental techniques, such as analysis of point mutations, generation of chimeric receptors, and alanine or cysteine scanning.[24–27] As a result, it is now accepted that class A GPCRs dimerize through transmembrane (TM) helices contacts, and different interfaces have been suggested for different homo- or heteroaggregates.[11,24–27] Molecular dynamics techniques and normal-mode analysis have also been employed as a tool to investigate the dynamics and the mutual accommodation of protomers to assemble the dimer.[28,29] In this paper, we report the generation of a 3D model of the dimeric assembly between the transmembrane regions of mGluR2 and $5HT_{2A}$. According to the original report by Gonzales-Maeso et al.,[11] the dimerization occurs through transmembrane helices 4 and 5 (TM4 and TM5, respectively), in a $TM4_{mGluR2}$-$TM5_{5HT2A}$/$TM5_{mGluR2}$-$TM4_{5HT2A}$ arrangement. The dimer was therefore constructed by assembling a TM4/TM5 interface, and then it was embedded in an explicit phospholipidic bilayer (DMPC) and simulated for 40 ns through molecular dynamics (MD). In a separate experiment, the model of the $5HT_{2A}$ monomer was embedded in the same bilayer and simulated, under the same conditions, for 40 ns of MD. The two simulations were then compared, also by using essential dynamics analysis, and the differences between the dimer and the monomer are discussed. Finally, docking studies were tackled on selected frames of each MD simulation in order to test the influence of the heterodimerization on the binding mode of selected hallucinogen and nonhallucinogen ligands.

MATERIALS AND METHODS

i. Construction of the Two Protomers. The two protomers were constructed by homology modeling, starting from available templates. In particular, we chosen the recently disclosed structure of human β_2-adrenergic receptor (pdb code: 2RHI)[30] as a template for human $5HT_{2A}$, due to the close evolutionary relationship between the two receptors (both belonging to family A of GPCRs and both using a biogenic amine as transmitter). In the case of the transmembrane domain of mGluR2, we used the structure of bovine rhodopsin (pdb code: 1GZM)[31] as a template, since there are no clues indicating that the unrelated β_2-adrenergic or A_{2A} adenosine receptors could be better templates for family C GPCRs, while 3D models built on the basis of the rhodopsin structure were already reported and partially validated.[11,32]

Thus, the two sequences of $5HT_{2A}$ and $\beta 2$ were aligned using the ClustalW server,[33] and the resulting alignment was consistent with that reported by Gonzalez-Maeso et al.[11] The 3D model of $5HT_{2A}$ was generated using the MOE-align tool of the suite Molecular Operating Environment (MOE).[34] The loops were built by the loop search method implemented in MOE. The resulting model had the conserved disulfide bond between C148 on TM3 and C227 on extracellular loop 2 (E2). The protonation state of ionizable residues was fixed by using Protonate3D tool of MOE and then checked by visual inspection. The geometry of the final model was optimized using a stepwise approach: first the internal strain of the model was reduced by manually modifying the rotamers of residues participating to steric clashes. Then, the structure was relaxed by using several cycles of Amber99 force field (available in MOE) minimization, until a gradient of 0.1 kcal/mol $Å^{-1}$ was reached.

For the construction of the model of the transmembrane region of human mGluR2 the following approach was used. First of all, the large amino terminal domain (ATD) was manually eliminated from the primary sequence (Expasy Q14416).[35] Then, the TM helices were aligned to the sequence of bovine rhodopsin (pdb code: 1GZM),[31] by reproducing the alignment reported by Gonzalez-Maeso et al.[11] However, the resulting model, built in MOE, lacked the disulfide bond between C632 on TM3 and C721 on E2 (numbering from the full length sequence of human mGluR2, expasy code Q14416). In a different approach, we reproduced the alignment between human mGluR1 and bovine rhodopsin, reported by Vanejevs et al.[32] The resulting 3D model of the transmembrane region of mGluR1 was then used as a template for the construction of the 3D model of the highly conserved mGluR2, which, now, showed the TM3-E2

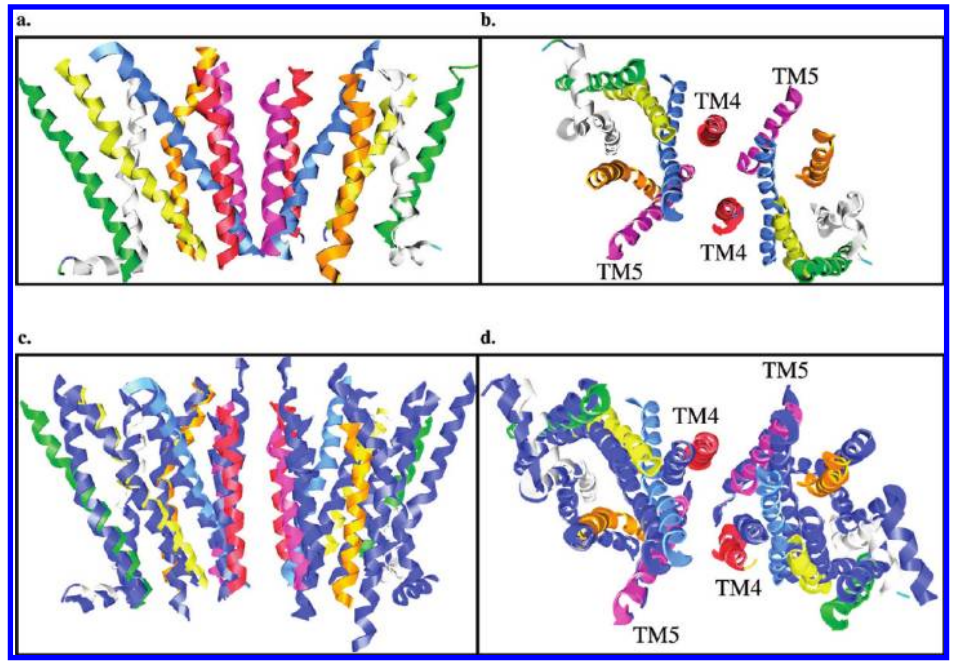

Figure 1. Final model of the heterocomplex. (a) Side view, $5HT_{2A}$ left, mGluR2 right. TM1 helices are colored in green, TM2 in yellow, TM3 in blue, TM4 helices are colored in red, TM5 helices are colored in purple, TM6 in orange and TM7-Helix8 in white. (b) Top view from the intracellular side. Position and colors are as above. (c) Side view and (d) top view of the heterocomplex superimposed to the theoretical model of the rhodopsin homodimer, in blue. Positions and colors are as above.

disulfide bond. The models of the transmembrane regions of mGluR1 and mGluR2 were generated by using the same tools, procedures, and protocols described above for $5HT_{2A}$.

ii. Construction of the Heterodimer Complex. The model of the heterodimer complex was generated by using Rosetta^{++}.[36,37] Rosetta works by simultaneously optimizing the side-chain conformation and the rigid body position of the two docking partners. In our present case we have used the "blind docking" tool present in Rosetta, thus performing a global random rigid-backbone docking. Before the docking was performed, the side-chain prepacking was carried out as implemented in the Rosetta side chain packing algorithm to prevent errors in docking due to irregularities. After that, a docking with a full atom, high-resolution search protocol was carried out. A simple Coulombic potential with distance-dependent dielectric was used (only aromatic−aromatic, aromatic−charged, and charged−charged interactions are considered). Finally 50 cycles of Monte-Carlo minimization were used to optimize the resulting complexes. In a calibration study carried out on the theoretical model of rhodopsin homodimer (pdb code: 1N3M) by Pacelwski et al.,[24,25] starting from two monomers of rhodopsin, we observed that energetic scores could not correctly sort out the output models (Tables 1S-3S, Supporting Information). Thus, the Rosetta^{++} outputs were scored and sorted according to visual inspection and rmsd matrix (Table 1S, Supporting Information). More in details, in the case of the mGluR2/$5HT_{2A}$ heterodimer, we visually selected only those models owing a TM4/TM5 interface, and, among them, the ranking was manually performed by using as reference parameters the distance between the monomer, the angle of interaction, and the alignment between the top and bottom edge of the receptors, in such a way as to match as much as possible those found in the 1N3M homodimer structure. The final model of the heterocomplex is shown in Figure 1.

iii. Molecular Systems. The mGluR2-$5HT_{2A}$ dimer and, separately, the $5HT_{2A}$ monomer were embedded in explicit phospholipid bilayers resembling a cellular membrane environment (Figure 2). For this purpose, the *Membrane Builder* tool in the Charmm-gui.org server was used, by employing the 'replacement method' for the construction of the bilayer.[38–40] For both systems, a dimyristoylphosphatidylcholine (DMPC)-based bilayer was generated in a rectangular water box in which the ionic strength was kept at 0.15 M by KCl. The overall charge of both systems was automatically neutralized by the *Membrane Builder* tool. Table 1 lists the characteristics of both systems. Among the several output files generated by the Charmm-gui.org server, there are the topology files that we used for the subsequent molecular dynamic simulations.

iv. Molecular Dynamics Simulations. Molecular dynamic simulations were carried out using NAMD2.6[41] and using Charmm22/27 as force field,[42] and the results were analyzed with VMD.[43] The two models were first separately equilibrated in a NVT system by following the protocols depicted in Table 2.

The harmonic constraints were progressively reduced during the equilibration to achieve a smooth relaxation of the assembly. The last 250 ps were carried out with no constraints. The simulations were then carried out, separately, in a NPT system, by imposing a pressure target value of 1.01325 bar (see Table 2). Both simulations were carried out with the same nonbonded interaction parameters (van der Waals and nonbonded electrostatic interactions); a cutoff of 16 Å was imposed for nonbonded interactions, and a smooth switching function was used to truncate the van der Waals potential energy smoothly at the cutoff distance; the parameters that specifies the distance at which the switching function should start was set to 14 Å. The nonbonded electrostatic interactions are truncated at the same cutoff

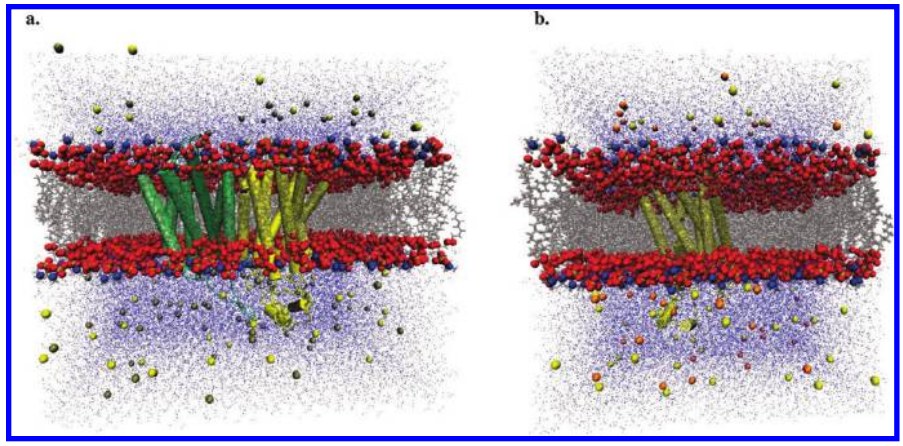

Figure 2. Final molecular systems before the MD equilibration and simulation. (a) Heterocomplex (lime: mGluR2, yellow: $5HT_{2A}$) and (b) monomeric $5HT_{2A}$ (yellow), embedded in a phospolipidic (DMPC) bilayer (red (O), blue (N), and dark yellow (P) represent the polar heads, while transparent gray represents the hydrophobic tail of the lipids), surrounded by a rectangular box of TIP3 water molecules (blue). In different yellow scales, K+/Cl- ions are depicted.

Table 1. Parameters Used for the Embedding of the Heterocomplex and of the $5HT_{2A}$ Monomer into the Phospholipidic Bilayer

	membrane-receptor complexes					
	mGluR2-$5HT_{2A}$			$5HT_{2A}$		
Box type	rectangle			rectangle		
System size	x	y	z	x	y	z
	118.863	96.3427	103.672	94.9372	94.9372	104.583
Crystal angle	α	*β*	*γ*	α	*β*	*γ*
	90.0	90.0	90.0	90.0	90.0	90.0
Number of lipids	307			257		
System building options	replacement method			replacement method		
	water box	include ions (0.15 M KCl)		water box	include ions (0.15 M KCl)	
Number of atoms	123079			97004		
Number of waters	25816			20429		
Lipids	DMPC			DMPC		

Table 2. Parameters Used for the MD Equilibration and Production Phases

				harmonic constraints (kcal/mol)					
	timestep	numstep	temperature	backbone	side chains	lipids	waters	ions	constant temperature control
				Equilibrations Steps					
Step1	1.0 fs	2500 fs	300 K	50	50	50	50	50	NVT
Step2	1.0 fs	2500 fs	300 K	10	10	10	5	5	NVT
Step3	1.0 fs	5000 fs	310 K	10	10	10	5	5	NVT
Step4	1.0 fs	5000 fs	310 K	10	5	10	5	5	NVT
Step5	1.0 fs	25000 fs	310 K	2.5	2.5	2.5	1.0	1.0	NVT
Step6	1.0 fs	25000 fs	310 K	2.5	1	2.5	1	2.5	NVT
Step7	1.0 fs	25000 fs	310 K	-	-	-	-	-	NVT
				Simulation					
Step7	1.0 fs	40 ns	310 K	-	-	-	-	-	NPT $P = 1.01325$ bar

value for the van der Waal interactions with the same switchdist value. Moreover we used a nonbonded pair list with a '*pairlistdist*' parameter set to 18 Å. The periodic boundary conditions were set by using the system size shown in Table 1 as reference. The two simulations were conducted for 40 ns each, with an integration step of 1 fs.

v. Molecular Dynamics Analysis. The trajectories were analyzed with VMD. An Essential Dynamics (ED) analysis was performed by using the appropriate VMD plug-in in combination with the ptraj module of Amber9.[43–45] ED allows identification of a new essential subspace of coordinates by the diagonalization of the covariance matrix of atomic fluctuations. For a $X_{(t)}$ multidimensioned system, where X could be a system of spatial coordinates, frames of molecular dynamics simulations, etc., we could obtain the following covariance matrix:

$$C_{ij} = \langle (x_i - \langle x_i \rangle)(x_j - \langle x_j \rangle) \rangle$$

The symmetric matrix can be diagonalized by an orthonormal transformation matrix, which contains the eigenvectors or principal modes (columns of the matrix) and where the eigenvalues λ express the variance in the direction of the corresponding eigenvector. Every eigenvector is stored, in decreasing way, on the basis of the corresponding eigenvalue. So for a dynamic process the original data can be projected onto an eigenvector and the eigenvectors with larger eigenvalues match the more important displacement.[46–48]

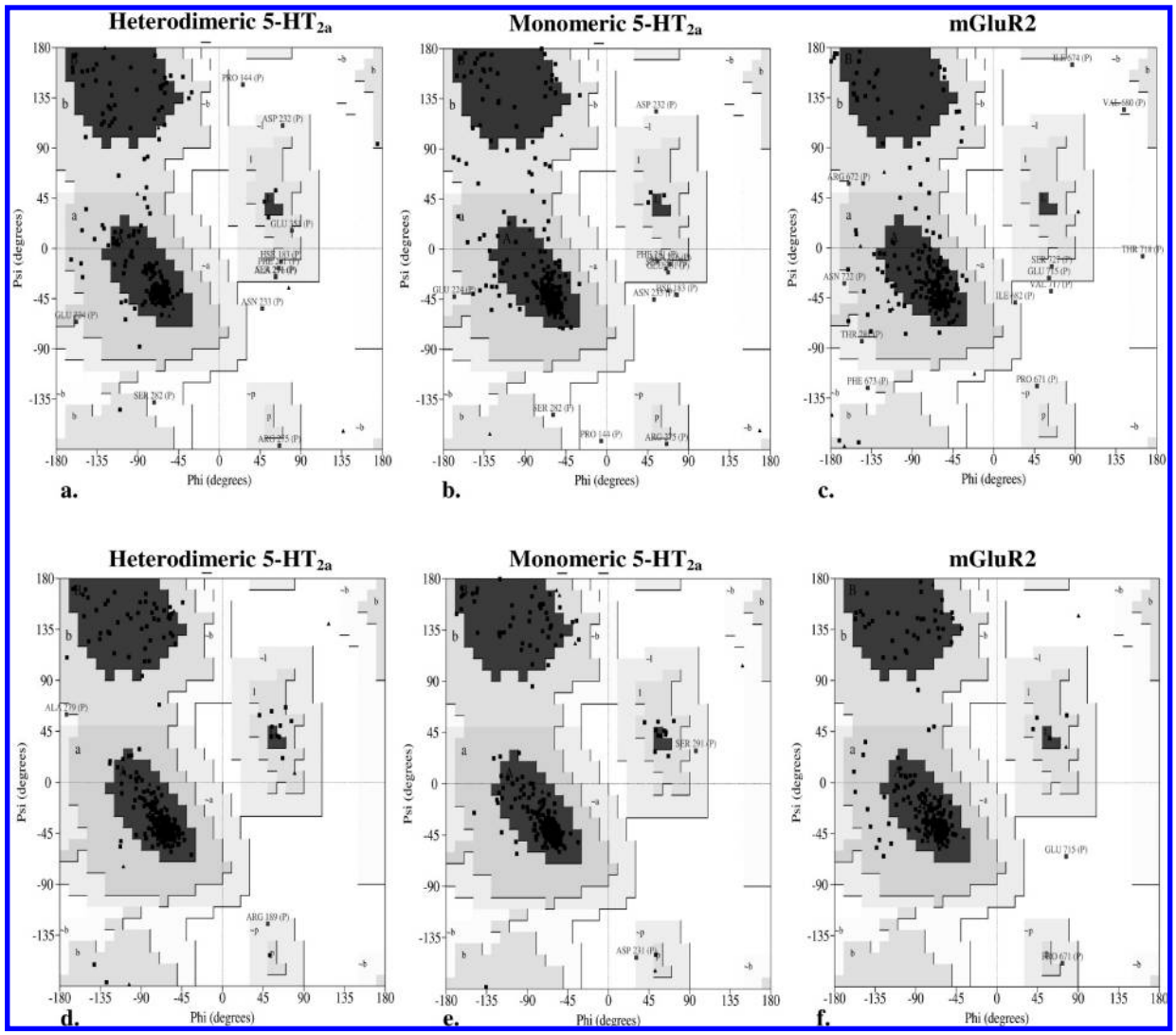

Figure 3. Ramachandran plots before (a-c) and after (d-f) MD simulation for the two protomers extracted from the heterocomplex (a,c and d, f) and for the monomeric $5HT_{2A}$ receptor (b and e).

After removing the roto-translational degree of freedom by aligning every frame of the two simulations on a reference structure, the principal modes were computed for the Cα atoms only.

vi. Docking Studies. Docking studies were performed by using the AutoDock Vina program.[49] This version of Autodock uses as input files the 3D coordinates of both ligand and receptor, which must be converted into the appropriate format by using the ADT program.[50] The 3D structure of LSD (**3**) was taken from the crystal structure.[51,52] Ligands needed for docking experiments were prepared within Sybyl.[53] In the case of LSD, hydrogen atoms were added to the crystallographic coordinates, and the resulting structure was minimized in order to relax the tension due to the stretching and bending energies. Serotonine structure was constructed from Sybyl fragment libraries, and the geometry was further optimized. Ligands structures were read by the ADT program, nonpolar hydrogens were deleted, and rotatable bonds were defined. Finally, the structure was saved in the appropriate format to be used with AutoDock program.

The homology model of the $5HT_{2A}$ and the structures selected from the MD simulations were prepared for docking experiments by using the ADT program. Nonpolar hydrogen atoms were deleted and charges were added to the structure, which was saved in the appropriated format. A cubic grid with a 16 Å side, centered on the $5HT_{2A}$ binding site, needed for docking, and one docking run was performed on each receptor structure.

RESULTS

i. Analysis of the Stability of the Models. The two molecular systems constituted by the dimeric assembly and by the $5HT_{2A}$ monomer, respectively, embedded in a rectangular box comprising a DMPC bilayer surrounded by explicit water were simulated for 40 ns each, and the stability of the systems was evaluated by monitoring several parameters. The temperature and the volume of the two molecular systems were stable in the NTP ensemble after equilibration, keeping around values of $T = 310.28 \pm 3.32$ K and $V = 1166847.00 \pm 6118.00$ A^3 for the dimer, and $T = 309.25 \pm 6.97$ K and $V = 919791.19 \pm 8248.87$ A^3 for the $5HT_{2A}$ monomer, respectively. Figure 3 shows the Ramachandran plots for the two monomeric protomers and the monomer before (Figure 3a-c) and after (Figure 3d-f) the molecular dynamics simulations, indicating an excellent conservation of the secondary structure elements during the simulation.

The root-mean-square deviations (rmsd) of the Cα of the two protomers constituting the dimer were computed against

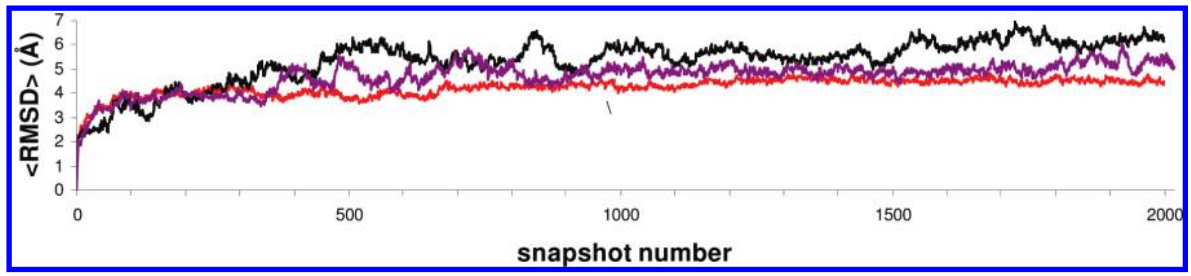

Figure 4. Root mean square deviation (rmsd) of the Cα atoms for $5HT_{2A}$ (black) and mGluR2 (red) protomers extracted from the hetercomplex and for monomeric $5HT_{2A}$ (purple).

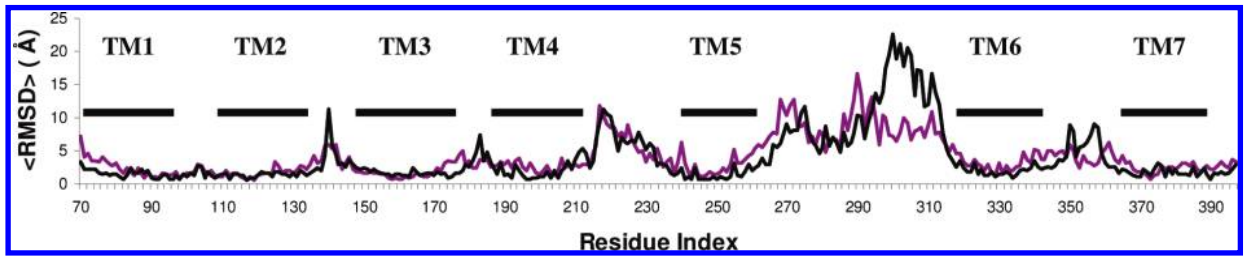

Figure 5. Average rms fluctuation per residue for $5HT_{2A}$ as a protomer in the heterocomplex (black) and as monomer (purple). Horizontal bars depict the TM domains.

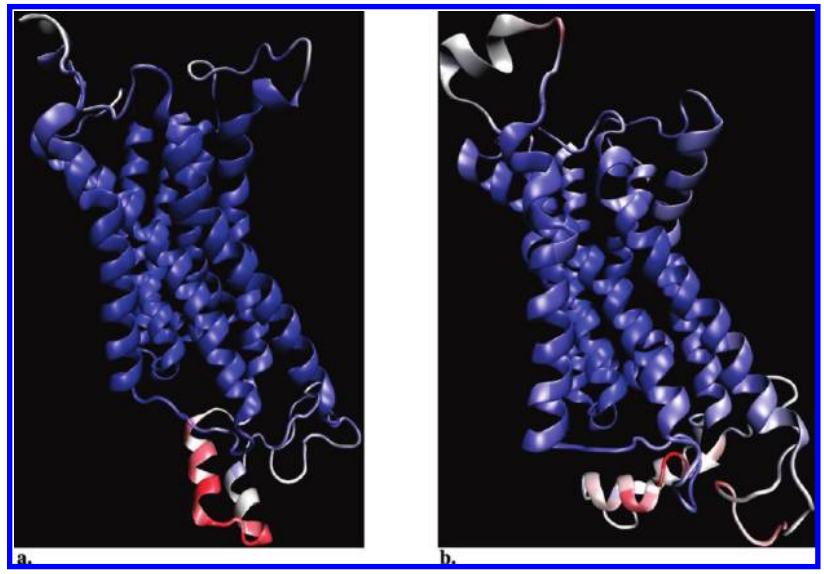

Figure 6. 3D ribbon representation of $5HT_{2A}$ as a protomer of the heterocomplex (a) and as monomer (b), colored according to rmsd of Cα atoms. Dark blue: lowest rmsd from the starting structure; red: highest rmsd from the starting structure.

the starting structures and are reported in Figure 4. In the same figure, the rmsd of the Cα of the monomeric $5HT_{2A}$ simulation is also reported. It can be appreciated that the two protomers behave differently as the mGluR2 unit (red line) has a lower deviation from the starting structure than the $5HT_{2A}$ protomer (black line). Interestingly, when simulated in a monomeric form (purple line), the $5HT_{2A}$ unit has a lower deviation from the same starting structure than the protomer in the dimeric complex (black line).

However, inspection of the plot of the rms fluctuation per residue, along the simulations, revealed a more complex picture. Indeed, when the two $5HT_{2A}$ models (the monomer, purple line and the protomer, black line, respectively) are compared (Figure 5), it appears that residues belonging to TM1-TM3 have almost identical fluctuations, while modest differences are visible for residues belonging to TM4-TM7, with the monomer endowed with higher fluctuations.

Most of the variance, however, is due to loop movements, and in particular of the C-terminus of the third intracellular loop, where the protomer of the heterodimer has the highest fluctuations. This is due to the mutual accommodation of the large third intracellular loops in the dimer, an effect which is not apparent in the monomer, where there are no interprotomer contacts to be relaxed (Figure 6).

In the case of the mGluR2 protomer, again, there is a major fluctuation associated with the second intracellular loop, and, interestingly, residues belonging to TM domains have higher fluctuation when compared to the $5HT_{2A}$ models. This is confirmed by the analysis of the rmsd of the Cα for the TM domains of the three models (Figure 7a-g).

The comparison between the rmsd of the Cα of the two $5HT_{2A}$ models suggests the presence of a clear effect of the dimerization interface. Indeed, the rmsd of Cα belonging to TM1 and TM2, not involved in the interface, are almost identical in the two cases. Minor deviations are visible for residues belonging to TM3 and TM4, while significant differences occurred in the case of residues belonging to TM5, TM6, and TM7, thus clearly indicating that the

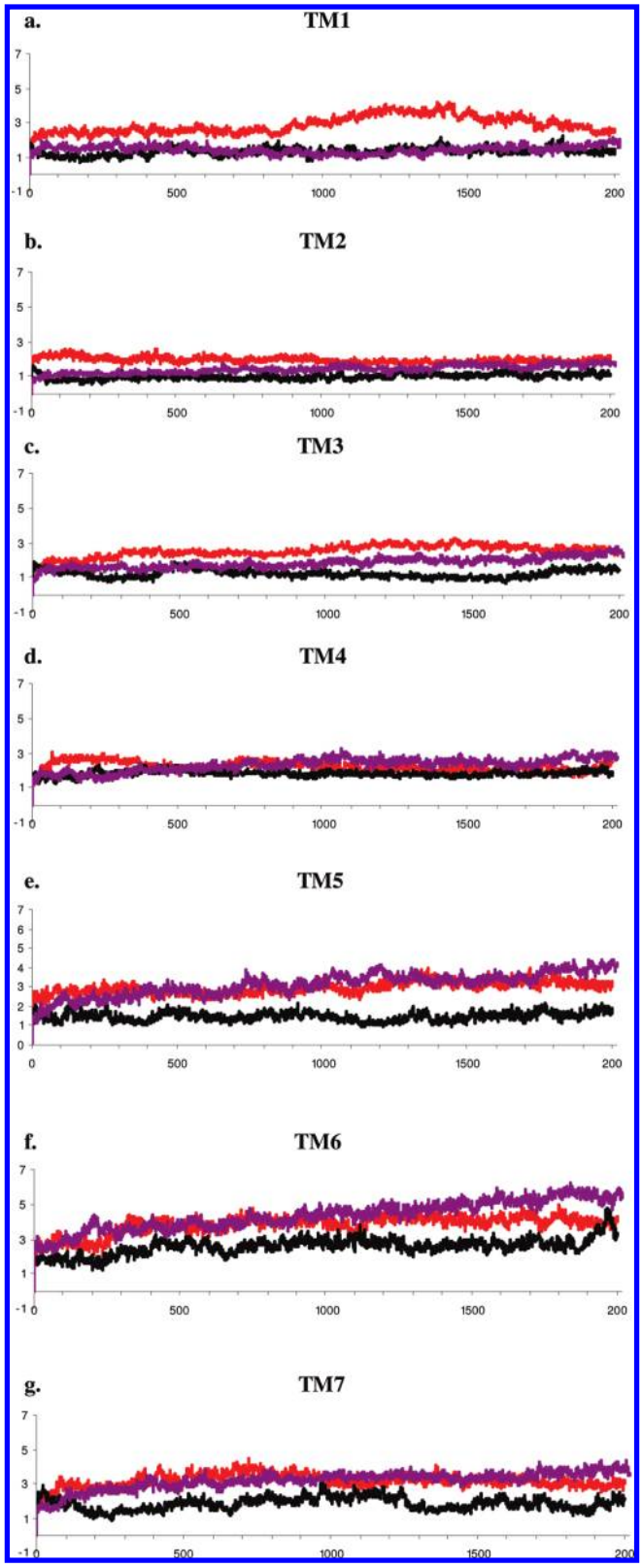

Figure 7. rmsd of Cα atoms of residues defining TM1-TM7 (a-g, respectively) for $5HT_{2A}$ (black) and mGluR2 (red) as protomers in the heterocomplex and for $5HT_{2A}$ (purple) as monomer.

presence of the dimerization interface impacts the result of the MD simulations.

ii. Essential Dynamics Analysis. Essential dynamics analysis was carried out to further assess the differences between the simulations of $5HT_{2A}$ as a monomer and as a protomer in the dimer complex. The internal motions of the systems were evaluated after removing the overall rotation and translational motion by overlapping the Cα atoms of each frame on those of the reference structure.[46,47] The first five principal components of the $5HT_{2A}$ receptor in heterodimer form and monomer form describe 87.1% and 85.9%, respectively, of the total motion. The essential space explored by the two systems along with the first two eigenvectors is reported in Figure 8.

iii. Analysis of the Dimerization Interface. According to Gonzales-Maeso et al.,[11] TM4-TM5 of both protomers form the dimerization interface. When the two protomers are docked together, the resulting TM4-TM5 interface appears to be constituted by a hydrophobic portion, comprising almost two-thirds of the membrane spanning domain from the extracellular side, and one smaller hydrophilic portion, located at the intracellular side (Figure 9).

In order to assess the stability of the proposed interface, the number of contacts during the simulation has been evaluated. According to the Essential Dynamics analysis of the trajectory (see below and Figure 8), two intervals of the simulation were selected covering two opposite regions in the essential space. These are the intervals between 10.4 and 11.4 ns and the last ns of the simulation. The analysis was carried out by setting a cutoff for contacts of 3.5 Å, and only residues of TM4 and TM5 of both protomers that are exposed to the dimerization interface were taken into account. In addition to interprotomer contacts, we have also analyzed the fluctuation of the distances between centers of mass of pairs of TM domains on the basis of the $TM4_{5HT2A}$-$TM5_{mGluR2}$/$TM5_{5HT2A}$-$TM4_{mGluR2}$ arrangement (Supporting Information, Figure 2-3S). For the $TM4_{5HT2A}$ the center of mass corresponds to the N atom of the $T^{4.51}$ (Weinstein-Ballesteros notation), while for $TM5_{5HT2A}$ the center of mass is the N atom of the $I^{5.53}$. For the mGluR2 receptor the respective center of mass are the N atom of $V^{4.51}$ ($TM4_{mGluR2}$) and the Cα atom of $L^{5.53}$ ($TM5_{mGluR2}$). We can define contacts between residues as follows: very frequent, when the contact is present in more than 70% of the analyzed frames; frequent, when the contact is present in a range between 70% and 40%; and occasional, when the contact is present in less than 40% of the frames.

As indicated in Table 3 the dimerization interface undertook significant rearrangement during the dynamic simulation. Indeed, the starting heterodimer complex, after minimization, had a total of 25 interprotomer contacts (of which, only one hydrogen bond). In the interval between 10.4 and 11.4 ns 31 different contacts are detected, of which 25 are very frequent, and 3 are frequent. In the last nanosecond, 37 independent contacts are detected of which 28 are very frequent, and 1 is frequent.

In the minimized starting heterocomplex, the distances between the centers of mass for $TM4_{5HT2A}$-$TM5_{mGluR2}$/$TM5_{5HT2A}$-$TM4_{mGluR2}$ were 8.09 and 9.4 Å, respectively. In the interval 10.4−11.4 ns these figures became 7.55 and 8.99 Å, respectively, and in the final nanosecond reached values of 7.95 and 8.51 Å, respectively (see Figure 2S-3S, Supporting Information).

The mutual accommodation of TM4 and TM5 domains of the two protomers during the simulation is further confirmed by the inspection of the van der Waals surfaces (probe radius 1.4 Å) of the initial minimized complex (Figure 10a), of a snapshot taken from the 10.4−11.4 ns interval

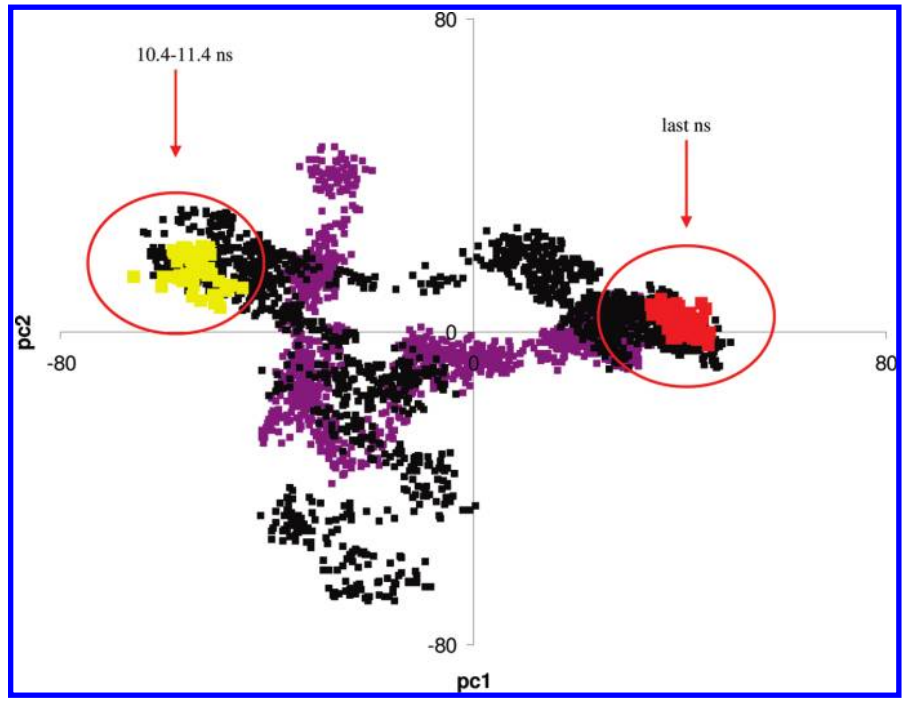

Figure 8. Essential space explored by 5HT$_{2A}$ (black) as a protomer in the heterocomplex and by 5HT$_{2A}$ (purple) as monomer, projected over the two first eigenvectors of the essential dynamics analysis. The interval between 10.4−11.4 ns and the last nanosecond of simulation are highlighted.

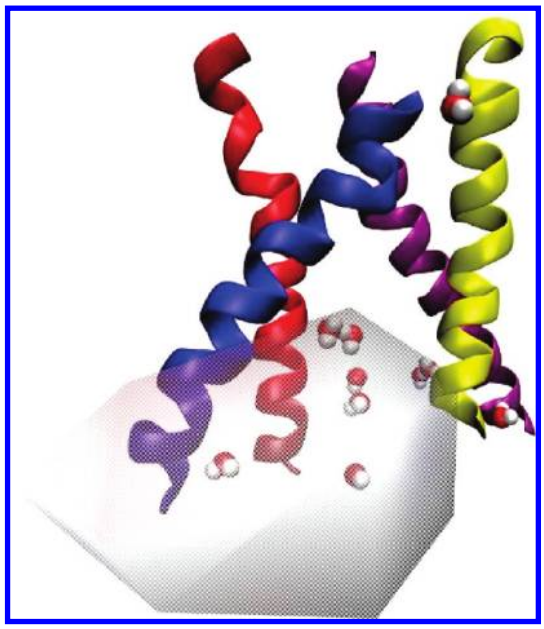

Figure 9. Close-up of the dimerization interface. In red, TM4 5HT$_{2A}$, in purple TM5 5HT$_{2A}$, while in blue TM5 mGluR2 and in yellow TM4 mGluR2. The hydrophilic domain, filled by water molecules, is highlighted on the bottom. Waters are depicted by VDW radii.

(Figure 10b) and of a snapshot taken from the last nanosecond interval (Figure 10c).

It can be appreciated that, during the simulation, the extracellular side of TM5 of mGluR2 bends over TM4 of the same protomer thus reducing its buried surface with respect to TM4 of 5HT$_{2A}$. Interestingly, this reduction correlates with an increase of the average number of contacts between the two protomers during the simulation.

iv. Analysis of the Binding Sites. A potentially very relevant outcome of the present study is the observation that the formation of the dimerization interface between the two protomers allosterically affects the shape of the binding pocket(s) of the individual protomers. In order to verify whether this allosteric cross-talk did actually occur, we analyzed the putative 5HT$_{2A}$ binding pocket, which is quite well-defined from previous experimental results.[54–60] In details, we followed seven residues known to be involved in 5HT$_{2A}$ ligand recognition, namely D$^{3.32}$, S$^{3.36}$, T$^{3.37}$, S$^{5.43}$, S$^{5.46}$, W$^{6.48}$, and Y$^{7.43}$. Figure 11a reports the rmsd of these residues for the protomer in the dimer simulation and for the monomer, respectively. Figure 11b shows the corresponding average rmsd fluctuation for the same residues. It can be appreciated that residues belonging to TM3 have an almost overlapping behavior, while significant deviations are detected between the two simulations for the key residues S$^{5.43}$, S$^{5.46}$, W$^{6.46}$, and Y$^{7.43}$.

It is tempting to link this result to the experimental observation that the formation of the dimer complex increases the affinity of hallucinogen compounds for 5-HT$_{2A}$ while the hallucinogen component is reduced by glutamatergic activation of the mGluR2 counterpart.[11] The thorough simulation of the behavior of hallucinogen and nonhallucinogen compounds at the dimeric complex requires a methodological approach involving ensemble docking and MD simulation in the presence of ligands, which is far beyond the scope this article. Furthermore, it should be recalled that the two 5HT$_{2A}$ and mGluR2 protomers were modeled on the basis of the resting (inactive) state of their respective templates and that these models could not be appropriate for simulating the affinity of agonists. Nevertheless, we deemed it appropriate to preliminarily investigate whether the observed modification on the shape of the 5HT$_{2A}$ binding pocket induced by the dimerization can actually allow for a better fit of hallucinogen versus nonhallucinogen compounds. At this aim, we designed a protocol involving (i) the sampling of the essential space covered by the two MD simulations and the selection of representative frames, for the dimer and for

Table 3. List of Contacts at the TM4/TM5 Interfaces[a]

interface contacts							
starting structure[(a)]		10.4−11.4 ns[(b)]			last ns[(c)]		
$TM4_{5HT2A}$	$TM5_{mGluR2}$	$TM4_{5HT2A}$	$TM5_{mGluR2}$	type of contact	$TM4_{5HT2A}$	$TM5_{mGluR2}$	type of contact
$I^{4.60}$	$S^{5.42}$	$T^{4.51}$	$L^{5.53}/L^{5.56}$	very frequent	$T^{4.51}$	$L^{5.53}/L^{5.56}$	very frequent
		$I^{4.47}$	$L^{5.56}/Y^{5.60}$		$I^{4.47}$	$L^{5.56}/Y^{5.60}$	
		$L^{4.44}$	$Y^{5.60}$		$L^{4.44}$	$Y^{5.60}$	
$P^{4.59}$	$L^{5.64}$	$I^{4.52}$	$L^{5.53}/Y^{5.49}$		$I^{4.52}$	$L^{5.53}/Y^{5.49}$	
		$A^{4.48}$	$L^{5.56}/L^{5.53}$		$A^{4.48}$	$L^{5.56}/L^{5.53}$	
		$I^{4.56}$	$L^{5.44}/L^{5.56}$		$I^{4.56}$	$L^{5.44}$	
$G^{4.55}$	$Y^{5.49}$	$G^{4.55}$	$Y^{5.49}$				
		$I^{4.56}$	$Y^{5.49}$		$P^{4.59}$	$L^{5.44}$	
$I^{4.52}$	$L^{5.53}/Y^{5.49}$	$L^{4.45}$	$L^{5.56}$		$G^{4.55}$	$Y^{5.49}$	
$T^{4.51}$	$L^{5.56}/L^{5.53}$	$P^{4.59}$	$L^{5.44}$	frequent	$P^{4.59}$	$L^{5.49}$	frequent
$L^{4.44}$	$L^{5.56}/Y^{5.60}$	$T^{4.51}$	$Y^{5.49}$	occasional	$T^{4.51}$	$Y^{5.49}/Y^{5.49}$	occasional
$T^{4.40}$	$Y^{5.60}$				$T^{4.40}$	$Y^{5.60}/T^{5.64}$	
$A^{4.48}$	$L^{5.53}$				$L^{4.44}$	$T^{5.64}$	
$I^{4.47}$	$L^{5.56}$						

interface contacts							
starting structure[(a)]		10.4−11.4 ns[(b)]			last ns[(c)]		
$TM5_{5HT2A}$	$TM4_{mGluR2}$	$TM5_{5HT2A}$	$TM4_{mGluR2}$	type of contact	$TM5_{5HT2A}$	$TM4_{mGluR2}$	type of contact
$I^{5.41}$	$L^{4.55}/A^{4.59}$	$I^{5.60}$	$Q^{4.47}$	very frequent	$I^{5.60}$	$Q^{4.47}$	very frequent
		$T^{5.57}$	$I^{4.44}/Q^{4.47}$		$F^{5.44}$	$V^{4.51}/L^{4.55}$	
		$I^{5.53}$	$I^{4.44}/Q^{4.47}/L^{4.48}$		$I^{5.41}$	$L^{4.55}/A^{4.59}$	
					$I^{5.53}$	$I^{4.54}/Q^{4.47}/L^{4.48}$	
		$I^{5.49}$	$L^{4.48}/V^{4.51}$		$I^{5.49}$	$L^{4.48}/V^{4.51}/L^{4.55}/V^{4.52}$	
		$V^{5.45}$	$L^{4.55}$		$V^{5.45}$	$L^{4.55}$	
$F^{5.44}$	$W^{4.54}/L^{4.55}$; $I^{5.53}$	$F^{5.44}$	$V^{4.51}/L^{4.55}$				
		$I^{5.41}$	$L^{4.55}$		$T^{5.57}$	$I^{4.44}/Q^{4.47}$	
		$I^{5.41}$	$A^{4.59}$	frequent			frequent
$V^{5.45}$	$L^{4.55}$	$I^{5.49}$	$L^{4.55}$				
$Q^{4.47}$	$L^{4.48}$	$F^{5.44}$	$W^{4.54}$	occasional	$F^{5.49}$	$V^{4.52}$	occasional
					$V^{5.45}$	$V^{4.52}$	
$I^{5.49}$	$L^{4.55}/V^{4.51}/V^{4.52}/L^{4.48}$				$F^{5.44}$	$W^{4.54}$	
$T^{5.57}$	$I^{4.44}$	$I^{5.53}$	$V^{4.51}$		$I^{5.53}$	$V^{4.44}$	
$L^{5.60}$	$I^{4.44}$						

[a] Pairwise contacts between residues belonging to TM4/TM5, in the starting structure (a), averaged in the 10.4−11.4 ns interval (b), and averaged in the last ns interval (c).

the monomer; (ii) the docking of LSD (**3**, Chart 1) and serotonin (**5**) into each frame; and (iii) analysis of the docking results compared with experimentally available data on interacting residues.

v. Docking of Compounds. According to the protocol described above, we selected four frames from each simulation (Figure 4S, Supporting Information), along with the refined homology model of the $5HT_{2A}$ monomer, and LSD (**3**) and serotonin (**5**), as representative for hallucinogen and nonhallucinogen $5HT_{2A}$ agonists, respectively, were selected for docking studies, carried out as described in the Materials and Methods section. The quality of the docking poses is evaluated on the basis of the coherence with available mutagenesis data rather than solely on the basis of the docking scores or energies. The best pose (Figure 12a) obtained for the hallucinogen compound LSD into the starting homology model of $5HT_{2A}$ is barely in agreement with mutagenesis data, as the protonated nitrogen is correctly interacting with $Asp^{3.32}$, and the indole nitrogen is disposed 3.55 Å away from the crucial $Ser^{5.46}$, reported to be crucial for LSD binding.[60]

Overall, the disposition of LSD is not optimal, as the ligand lies in the upper part of the pocket, almost at the boundary with the extracellular portion. When LSD is docked into individual frames extracted from the monomeric MD simulations, the situation did not change, as the ligand is always positioned at the top of the binding pocket, and only seldom a pose in which the indole nitrogen interacts with $Ser^{5.46}$ is obtained (Figure 12b). Conversely, the binding pocket of the heterodimeric complex appears much more suitable for accommodating LSD. Indeed, good poses could be identified in each selected frames from the heterodimeric MD simulation, showing that LSD is able to form salt-bridge with $Asp^{3.32}$ and to donate hydrogen bonds to $Ser^{5.46}$ through the indolic NH group (Figure 12c-e). In agreement with experimental data, the role of $Ser^{5.43}$ is not vital for LSD binding, being that the distance between the oxygen atom of $Ser^{5.43}$ and the indole nitrogen atom is always larger than 4 Å. It is stimulating to observe that serotonin, the natural, nonhallucinogen neurotransmitter, cannot be productively docked into the selected frames from the dimeric MD simulation, due to the reshaping of the binding pocket which apparently prevents the simultaneous interaction with $Asp^{3.32}$, $Ser^{5.43}$, and $Ser^{5.46}$ (Figure 12f).

These preliminary results seems to converge into the notion that the presence of the dimerization interface allosterically modifies the $5HT_{2A}$ binding pocket thus allowing a fitting accommodation of a hallucinogen compound such as LSD

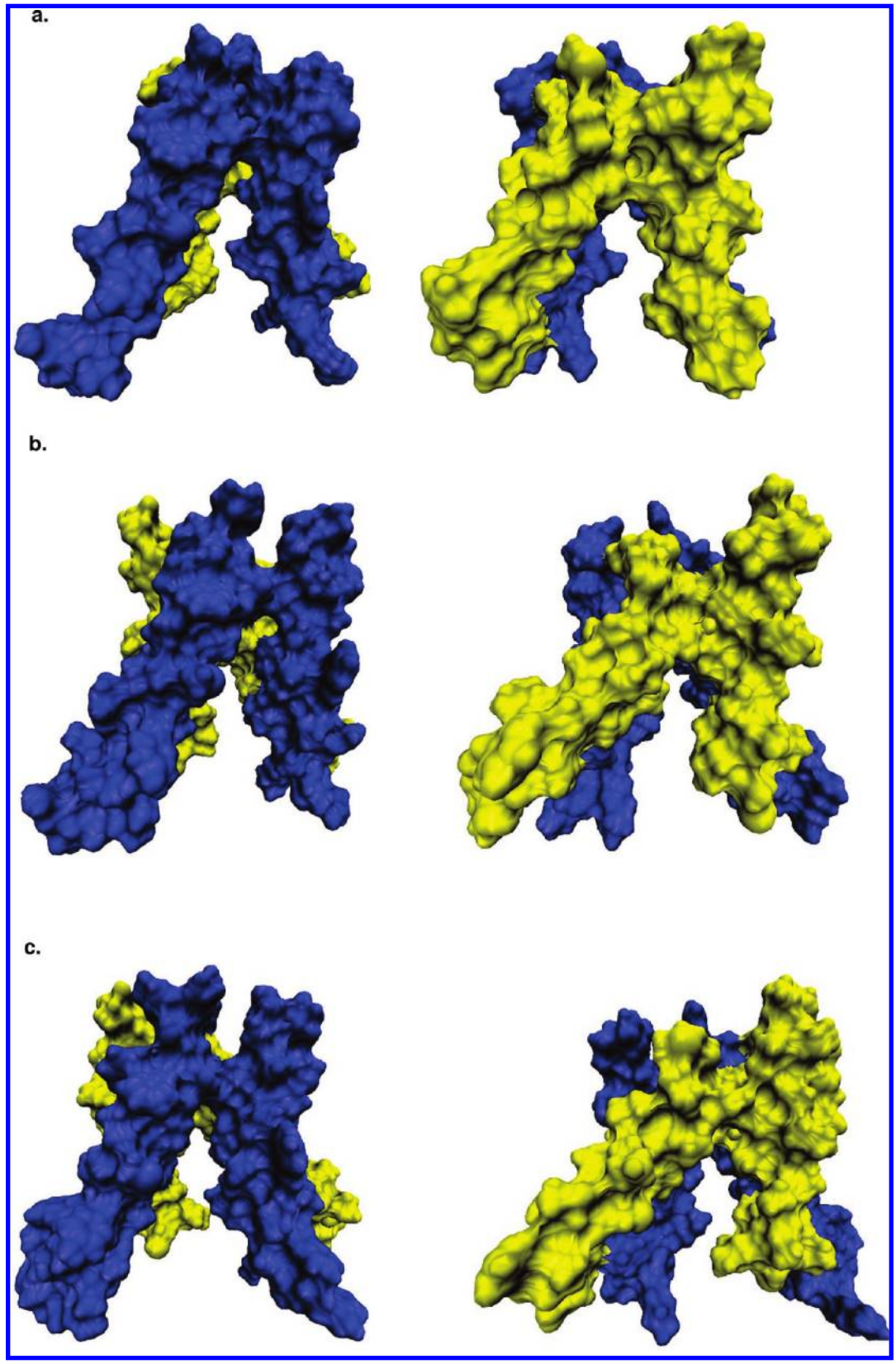

Figure 10. van der Waals surfaces (probe radius 1.4 Å) of the initial minimized complex (a), of a snapshot taken from the 10.4−11−4 ns interval (b), and of a snapshot taken from the last nanosecond interval (c). In the blue $5HT_{2A}$ side, while in the yellow mGluR2 side.

(**3**) while disfavoring the docking of serotonin (**5**). These data, however, should not be overemphasized at this stage, since a thorough study cannot disregard from the notion that the binding pocket of the monomeric $5HT_{2A}$, as deriving from homology modeling, is inherently tight and needs to be relaxed. What it should be stressed here is that the average shape of the binding pocket results significantly different whether the protomer is simulated alone or in a heteredimeric complex. From one side, this observation strongly supports the idea that dimerization allosterically influences ligand binding and that the interface can potentially transmit cross-talk between binding sites of the two protomers.[15,21] From

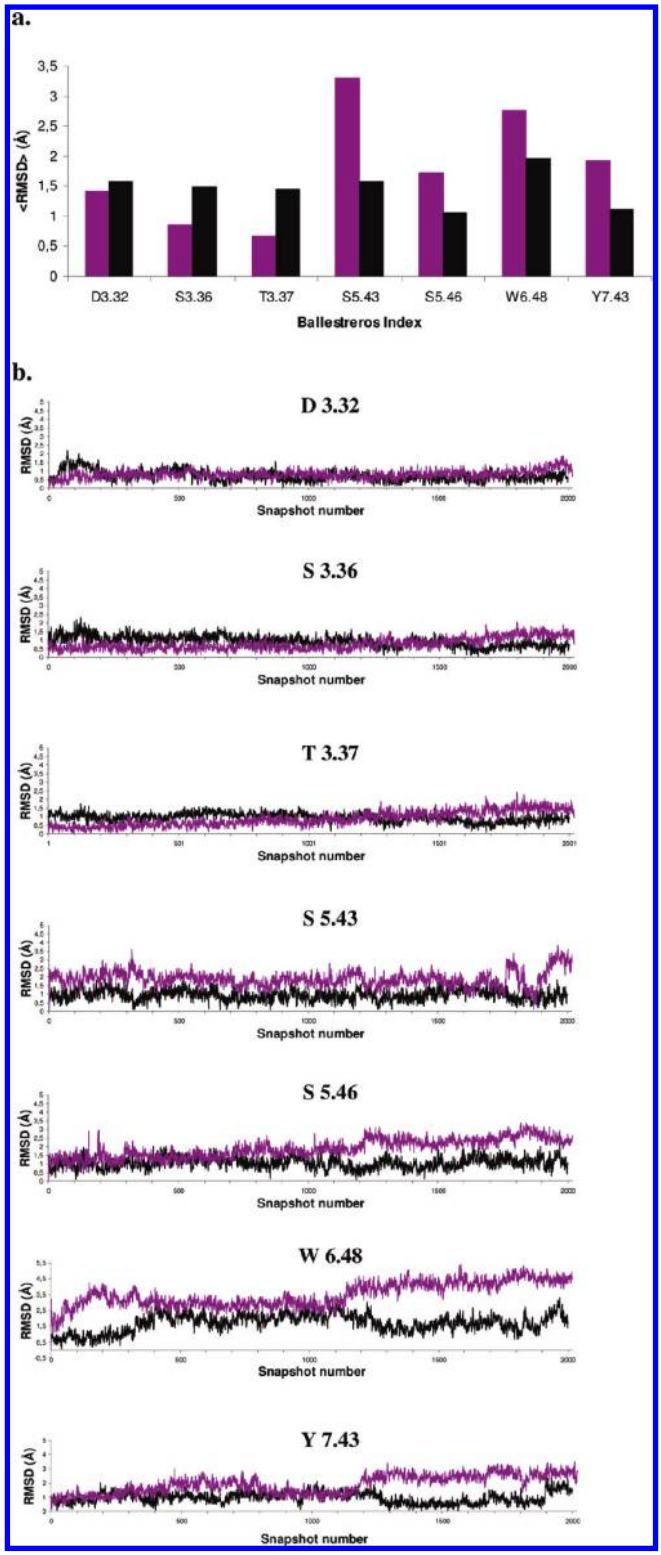

Figure 11. (a) Average rms fluctuations for the Cα atoms for selected residues lining up the binding pocket of $5HT_{2A}$. Black: protomer extracted from the heterocomplex; purple: monomer. Residues belonging to the monomer show higher displacement from the starting structure than those belonging to protomeric $5HT_{2A}$. (b) rmsd of Cα atoms for selected residues lining up the binding pocket of $5HT_{2A}$. In black: protomer extracted from the heterocomplex; in purple: monomer.

the other side, our results indicate that simulating a monomeric GPCR or the same GPCR in a dimer complex can yield significantly different results in terms of binding site topology, with potential recoils when using the models for docking or virtual screening.

DISCUSSION

A growing body of evidence indicates that GPCR may aggregate into homo- and heterodimers or oligomers. It was recently reported that two unrelated GPCRs, namely mGluR2 (belonging to class C GPCR) and $5HT_{2A}$ (belonging to class A GPRC), can form functional dimers and that the formation of the heterocomplex influences the hallucinogen signaling mediated by classes of serotoninergic agonists.[11] In this paper, we constructed and simulated by MD in an explicit DMPC bilayer a model of the heterocomplex between $5HT_{2A}$ and the transmembrane region of mGluR2, with the aim to gain insights into the stability of the construct and into the effect that the dimerization interface has on the topology of the putative binding pocket of individual protomers. In more detail, our study was focused to evaluate (i) the ability of constructing a stable interface, (ii) the stability of the construct in an explicit phospholipidic bilayer during 40 ns of simulation, and (iii) the effect of the dimerization in the shape of the binding pocket of $5HT_{2A}$. For comparison purposes, an identical MD simulation was carried out on the $5HT_{2A}$ monomer, embedded in the same DMPC bilayer.

According to experimental evidence, the heterocomplex was constructed by coupling the two protomers through a TM4/TM5 interface. The interface was initially assembled by rigid backbone docking, by using Rosetta^{++}, starting from models of the two protomers generated by homology modeling. As a kind of prevalidation, we have used the same protocol to reproduce the theoretical model of the rhodopsin homodimer, and it turned out that the scoring function was unable to correctly sort the interface disposition. We thus decided to visually sort the Rosetta^{++} output, and the selected interface was the one visually characterized as the most similar to the rhodopsin homodimer. The interface significantly changed during the MD simulation, leading to a number of modifications in hydrophobic microdomains which stabilized the complex. This brings support to the notion that rigid backbone docking is likely to yield a number of quasi-isonergetic dispositions of the protein−protein interface, which cannot be sorted out by scoring functions. This should be carefully taken into account when performing simulations of homo- or heterodimers of GPCR, since the choice of the initial structure may introduce a strong bias in the final results. In our present case, the choice was driven by the experimental evidence that the interface is made up of TM4/TM5, but among the several possible TM4/TM5 arrangements, the starting complex was selected based on visual inspection and coherence with the structure of a theoretical model of the rhodopsin homodimer[24,25] and not based on quantitative scoring. The energy minimization and the subsequent MD simulation demonstrated that the chosen interface is stable under the simulation conditions, but it cannot be ruled out that alternative disposition could have led to equally stable results. As additional control of the reliability of the chosen interface under our simulation conditions, we checked the occurrence of point mutations on residues exposed to the interface. Indeed, it is reported that chimeric mGluR2/R3 receptors, where TM4/TM5 of mGluR2 are substituted by the corresponding TM domains

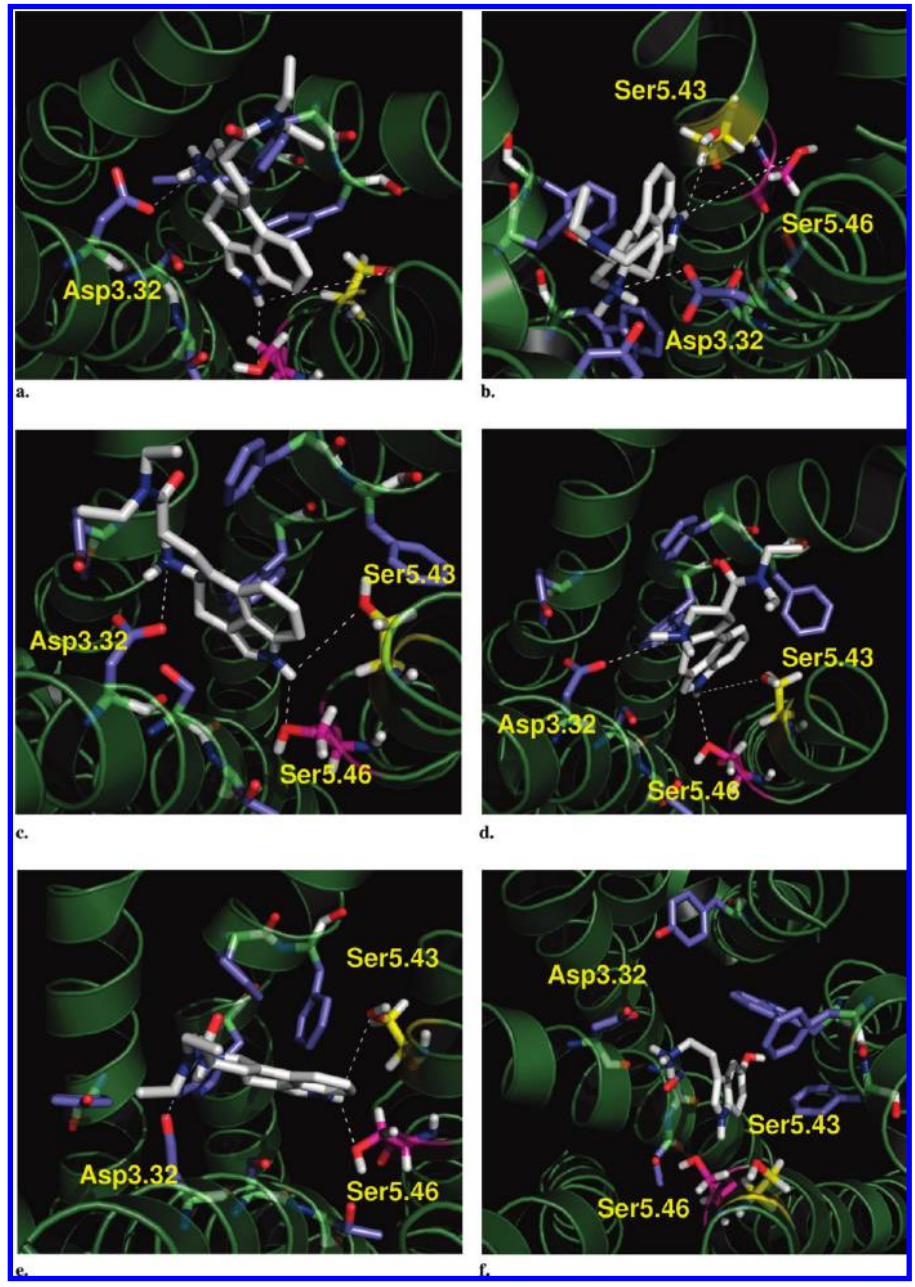

Figure 12. Results of the docking studies. Ligand (either LSD (**3**) or serotonin (**5**)) is colored according to atom types; Ser$^{5.46}$ is colored purple, Ser$^{5.43}$ is colored yellow, Asp$^{3.32}$ is colored dark blue. (a) Docking of LSD (**3**) into the refined homology model of 5HT$_{2A}$; (b) docking of LSD (**3**) into a representative frame (10 ns) of the monomeric MD simulation; and (c-e) docking of LSD (**3**) into representative frames (10, 20, 40 ns, respectively) of the heterodimeric MD simulation. The constant presence of a hydrogen bond between the indole nitrogen atom and Ser$^{5.46}$ can be appreciated. (f) Docking of serotonin (**5**) into a selected frame (20 ns) from the heterodimeric MD simulation. No interactions are visible with key residues.

of the homologous mGluR3, did not heterodimerize with 5HT$_{2A}$ when coexpressed in the same heterologous system.[11]

It is interesting to observe that TM4 and TM5 contain the largest number of mutations between mGluR2 and mGluR3 (TM4 10/24, TM5 8/26), and some of the mutated residues are those forming hydrophobic microdomains during simulation (Figure 13).

In particular, L$^{4.48}$ of mGluR2, which forms very frequent contacts in our simulation, is substituted by isoleucine in mGluR3. Also, V$^{4.52}$ in mGluR2 establishes a frequent contact in the last nanosecond of the simulation and is substituted by a serine in mGluR3. Q$^{4.47}$, which forms a very frequent hydrogen bond with T$^{5.57}$ of 5HT$_{2A}$ during the simulation, is conserved between mGluR2 and mGluR3, but it is surrounded by a cluster of mutations (S$^{4.45}$L, G$^{4.46}$V, L$^{4.48}$I, L$^{4.49}$V). Since the two transmembrane domains TM4 and TM5 are both necessary and sufficient for coprecipitation of mGluR2 and 5HT$_{2A}$ and can therefore be recognized as the specific domains for heterodimer formation,[11] it is intriguing to speculate that these point mutations may alter the ability of forming stable and/or functionally operative interface surfaces.

The heterocomplex was highly stable during the simulation, and both protomers maintained all the secondary structures elements. Nevertheless, when the 5HT$_{2A}$ protomer was simulated as a monomer under the same conditions of the heterodimer, some perceptible differences were noticed. While these differences can by no means be used, in our

Figure 13. Alignment of the TM domains of mGluR2 and mGluR3. Mutations are colored in blue, while those in bold are depicted in the residues of mGluR2 which are in contact with $5HT_{2A}$into the heterocomplex and the corresponding residues of mGluR3, in red the residues which correspond to the superconserved residues depend on the alignment with the bovine rhodopsin receptor.

opinion, to speculate about the functional role of the dimer, they clearly indicate that the presence of a dimerization interface does affect the outcome of the MD simulation on the topology of the individual protomers, and this has to be taken into account when using these models for in silico screening or docking purposes. This is particularly relevant in view of the observation that the mGluR2 component of the heterodimer affects the hallucinogen signaling operated by serotoninergic agonists. It can be speculated that the dimerization interface allosterically induces perceptible modifications on the shape of the $5HT_{2A}$ binding pocket, thus resulting in a modified affinity. Preliminary docking experiments seems to confirm this hypothesis, since selected frames from the heterodimeric MD simulation have an enlarged binding pocket and allow for a good accommodation of the hallucinogen compound LSD (3), in agreement with experimental data. Further and deeper studies are in progress, and the results will be communicated in due course, but we can anticipate that if this concept is proven, then the $5HT_{2A}$ binding pocket extracted from the equilibrated heterodimer should be considered as the target of choice for performing docking studies.

In conclusion, we have reported here a 40 ns simulation of the complex between the transmembrane regions of mGluR2 with the unrelated $5HT_{2A}$ in an explicit DMPC bilayer embedded in a rectangular water box. The scope of the simulation was not the generation of a mechanistic model of the mGluR2/$5HT_{2A}$ dimer. Indeed, limitations such as the lack of the Venus-flytrap domain of mGluRs (containing the orthosteric site for mGluR2 ligands), the use of models of the protomers based on the inactive state of GPCRs, and the lack of interacting G-proteins models severely prevent us to infer functional consequences from our models. Nevertheless, our results suggest a number of operational features that have to be taken into account when performing modeling experiments on GPCR dimerization. The first one is that the definition of the dimerization interface must be based to the largest possible extent on experimental evidence since methods based on energetic evaluation are likely to yield several degenerate outputs. The second important observation is that, at least in our system, the dimerization interface affects the topology of the binding site of individual protomers. This has potential relevance, since if the actual therapeutic target is the complex and not the individual monomer, then docking studies should be carried out on binding pockets extracted from the heterodimer.

ACKNOWLEDGMENT

G.C. acknowledges the University of Parma for financial support (FIL2007). A.E.G. acknowledges the Centro de Supercomputación de la Universidad de Granada Granada (CeSUG) for the generous allocation of computer time.

Supporting Information Available: Output of Rosetta^{++} docking (Table 1S−3S), alignment of $5HT_{2A}$ and mGluR2 transmembrane domain sequences on beta2 adrenergic (Figure 1Sa) and rhodopsin (Figure 1Sb), respectively, distances between centers of mass of TM4/TM5 during MD simulations (Figures 2S and S3), and selected frames from the two MD simulations used for the docking studies represented onto the essential dynamics space (Figure 4S).

This material is available free of charge via the Internet at http://pubs.acs.org.

REFERENCES AND NOTES

(1) Panetta, R.; Greenwood, M. T. Physiological relevance of GPCR oligomerization and its impact on drug discovery. *Drug Discovery Today* **2008**, *13*, 1059–1066.

(2) Dalrymple, M. B.; Pfleger, K. D.; Eidne, K. A. G protein-coupled receptor dimers: functional consequences, disease states and drug targets. *Pharmacol. Ther.* **2008**, *118*, 359–371.

(3) Milligan, G.; Smith, N. J. Allosteric modulation of heterodimeric G-protein-coupled receptors. *Trends Pharmacol. Sci.* **2007**, *28*, 615–620.

(4) Bayburt, T. H.; Leitz, A. J.; Xie, G.; Oprian, D. D.; Sligar, S. G. Transducin activation by nanoscale lipid bilayers containing one and two rhodopsins. *J. Biol. Chem.* **2007**, *282*, 14875–14881.

(5) Whorton, M. R.; Bokoch, M. P.; Rasmussen, S. G.; Huang, B.; Zare, R. N.; Kobilka, B.; Sunahara, R. K. A monomeric G protein-coupled receptor isolated in a high-density lipoprotein particle efficiently activates its G protein. *Proc. Natl. Acad. Sci. U. S. A.* **2007**, *104*, 7682–7687.

(6) Décaillot, F. M.; Rozenfeld, R.; Gupta, A.; Devi, L. A. Cell surface targeting of mu-delta opioid receptor heterodimers by RTP4. *Proc. Natl. Acad. Sci. U. S. A.* **2008**, *105*, 16045–16050.

(7) Marshall, F. H.; Jones, K. A.; Kaupman, K.; Bettler, B. GABAB receptors - the first 7TM heterodimers. *Trends Pharmacol. Sci.* **1999**, *20*, 396–399.

(8) Pin, J. P.; Galvez, T.; Prèzeau, L. Evolution, structure, and activation mechanism of family 3/C G-protein-coupled receptors. *Pharmacol. Ther.* **2003**, *98*, 325–354.

(9) Pin, J. P.; Kniazeff, J.; Binet, V.; Liu, J.; Maurel, D.; Galvez, T.; Duthey, B.; Havlickova, M.; Blahos, J. Prèzeau L.; Rondard, P. Activation mechanism of the heterodimeric GABA(B) receptor. *Biochem. Pharmacol.* **2004**, *68*, 1565–1572.

(10) Brock, C.; Oueslati, N.; Soler, S.; Boudier, L.; Rondard, P.; Pin, J. P. Activation of a dimeric metabotropic glutamate receptor by intersubunit rearrangement. *J. Biol. Chem.* **2007**, *282*, 33000–33008.

(11) Gonzàlez-Maeso, J.; Ang, R. L.; Yuen, T.; Chan, P.; Weisstaub, N. V.; Lòpez-Gimènez, J. F.; Zhou, M.; Okawa, Y.; Callado, L. F.; Milligan, G.; Gingrich, J. A.; Filizola, M.; Meana, J. J.; Sealfon, S. C. Identification of a serotonin/glutamate receptor complex implicated in psychosis. *Nature* **2008**, *452*, 93–97.

(12) Rorick-Kehn, L. M.; Johnson, B. G.; Burkey, J. L.; Wright, R. A.; Calligaro, D. O.; Marek, G. J.; Nisenbaum, E. S.; Catlow, J. T.; Kingston, A. E.; Giera, D. D.; Herin, M. F.; Monn, J. A.; McKinzie, D. L.; Schoepp, D. D. Pharmacological and pharmacokinetic properties of a structurally novel, potent, and selective metabotropic glutamate 2/3 receptor agonist: in vitro characterization of agonist (-)-(1R,4S,5S,6S)-4-amino-2-sulfonylbicyclo[3.1.0]-hexane-4,6-dicarboxylic acid (LY404039). *J. Pharmacol. Exp. Ther.* **2007**, *321*, 308–317.

(13) Conn, P. J.; Lindsley, C. W.; Jones, C. K. Activation of metabotropic glutamate receptors as a novel approach for the treatment of schizophrenia. *Trends Pharmacol. Sci.* **2009**, *30*, 25–31.

(14) Gonzàlez-Maeso, J.; Weisstaub, N. V.; Zhou, M.; Chan, P.; Ivic, L.; Ang, R.; Lira, A.; Bradley-Moore, M.; Ge, Y.; Zhou, Q.; Sealfon, S. C.; Gingrich, J. A. Hallucinogens recruit specific cortical 5-HT(2A) receptor-mediated signaling pathways to affect behaviour. *Neuron* **2007**, *53*, 439–452.

(15) Charles, A. C.; Mostovskaya, N.; Asas, K.; Evans, C. J.; Dankovich, M. L.; Hales, T. G. Coexpression of delta-opioid receptors with micro receptors in GH3 cells changes the functional response to micro agonists from inhibitory to excitatory. *Mol. Pharmacol.* **2003**, *63*, 89–95.

(16) Berthouze, M.; Rivail, L.; Lucas, A.; Ayoub, M. A.; Russo, O.; Sicsic, S.; Fischmeister, R.; Berque-Bestel, I.; Jockers, R.; Lezoualc'h, F. Two transmembrane Cys residues are involved in $5\text{-}HT_4$ receptor dimerization. *Biochem. Biophys. Res. Commun.* **2007**, *356*, 642–647.

(17) Parravicini, C.; Ranghino, G.; Abbracchio, M. P.; Fantucci, P. GPR17: molecular modeling and dynamics studies of the 3-D structure and purinergic ligand binding features in comparison with P2Y receptors. *BMC Bioinf.* **2008**, *9*, 263–271.

(18) Moro, S.; Spalluto, G.; Jacobson, K. A. Techniques: Recent developments in computer-aided engineering of GPCR ligands using the human adenosine A3 receptor as an example. *Trends Pharmacol. Sci.* **2005**, *26*, 44–51.

(19) Reggio, P. H. Computational methods in drug design: modeling G protein-coupled receptor monomers, dimers, and oligomers. *AAPS J.* **2006**, *8*, E322–336.

(20) Costanzi, S. On the applicability of GPCR homology models to computer-aided drug discovery: a comparison between in silico and crystal structures of the beta2-adrenergic receptor. *J. Med. Chem.* **2008**, *51*, 2907–2914.

(21) Damian, M.; Martin, A.; Mesnier, D.; Pin, J. P.; Banères, J. L. Asymmetric conformational changes in a GPCR dimer controlled by G-proteins. *EMBO J.* **2006**, *25*, 5693–5702.

(22) Levoye, A.; Dam, J.; Ayoub, M. A.; Guillaume, J. L.; Couturier, C.; Delagrange, P.; Jockers, R. The orphan GPR50 receptor specifically inhibits MT1 melatonin receptor function through heterodimerization. *EMBO J.* **2006**, *25*, 3012–3023.

(23) Snyder, S. H. Neuroscience: a complex in psychosis. *Nature* **2008**, *452*, 38–39.

(24) Liang, Y.; Fotiadis, D.; Filipek, S.; Saperstein, D. A.; Palczewski, K.; Engel, A. Organization of the G protein-coupled receptors rhodopsin and opsin in native membranes. *J. Biol. Chem.* **2003**, *278*, 21655–21662.

(25) Kota, P.; Reeves, P. J.; Rajbhandary, U. L.; Khorana, H. G. Opsin is present as dimers in COS1 cells: identification of amino acids at the dimeric interface. *Proc. Natl. Acad. Sci. U.S.A.* **2006**, *103*, 3054–3059.

(26) Guo, W.; Shi, L.; Filizola, M.; Weinstein, H.; Javitch, J. A. Crosstalk in G protein-coupled receptors: changes at the transmembrane homodimer interface determine activation. *Proc. Natl. Acad. Sci. U.S.A.* **2005**, *102*, 17495–17500.

(27) Guo, W.; Urizar, E.; Kralikova, M.; Mobarec, J. C.; Shi, L.; Filizola, M.; Javitch, J. A. Dopamine D2 receptors form higher order oligomers at physiological expression levels. *EMBO J.* **2008**, *27*, 2293–2304.

(28) Niv, M. Y.; Filizola, M. Influence of oligomerization on the dynamics of G-protein coupled receptors as assessed by normal mode analysis. *Proteins* **2008**, *71*, 575–586.

(29) Filizola, M.; Wang, S. X.; Weinstein, H. Dynamic models of G-protein coupled receptor dimers: indications of asymmetry in the rhodopsin dimer from molecular dynamics simulations in a POPC bilayer. *J. Comput.-Aided Mol. Des.* **2006**, *20*, 405–416.

(30) Cherezov, V.; Rosenbaum, D. M.; Hanson, M. A.; Rasmussen, S. G.; Thian, F. S.; Kobilka, T. S.; Choi, H. J.; Kuhn, P.; Weis, W. I.; Kobilka, B. K.; Stevens, R. C. High-resolution crystal structure of an engineered human beta2-adrenergic G protein-coupled receptor. *Science* **2007**, *318*, 1258–1265.

(31) Li, J.; Edwards, P. C.; Burghammer, M.; Villa, C.; Schertler, G. F. Structure of bovine rhodopsin in a trigonal crystal form. *J. Mol. Biol.* **2004**, *343*, 1409–1438.

(32) Vanejevs, M.; Jatzke, C.; Renner, S.; Müller, S.; Hechenberger, M.; Bauer, T.; Klochkova, A.; Pyatkin, I.; Kazyulkin, D.; Aksenova, E.; Shulepin, S.; Timonina, O.; Haasis, A.; Gutcaits, A.; Parsons, C. G.; Kauss, V.; Weil, T. Positive and negative modulation of group I metabotropic glutamate receptors. *J. Med. Chem.* **2008**, *51*, 634–647.

(33) Larkin, M. A.; Blackshields, G.; Brown, N. P.; Chenna, R.; McGettigan, P. A.; McWilliam, H.; Valentin, F.; Wallace, I. M.; Wilm, A.; Lopez, R.; Thompson, J. D.; Gibson, T. J.; Higgins, D. G. Clustal W and Clustal X version 2.0. *Bioinformatics* **2007**, *23*, 2947–2948.

(34) Chemical Computing Group. Scalable software Scalable Science. http://www.chemcomp.com (accessed Nov 3, 2008).

(35) Swiss Institute of Bioinformatics. ExPASy Proteomics Server. http://www.expasy.org (accessed Jun 26, 2008).

(36) Gray, J. J.; Moughon, S.; Wang, C.; Schueler-Furman, O.; Kuhlman, B.; Rohl, C. A.; Baker, D. Protein-protein docking with simultaneous optimization of rigid-body displacement and side-chain conformations. *J. Mol. Biol.* **2003**, *331*, 281–299.

(37) Center for Structural Biology, Yale University. ROSETTA++ http://www.csb.yale.edu/userguides7datamanip/rosetta/rosetta_descrip.html (accessed Jun 10, 2008).

(38) Jo, S.; Kim, T.; Iyer, V. G.; Im, W. CHARMM-GUI: a web-based graphical user interface for CHARMM. *J. Comput. Chem.* **2008**, *29*, 1859–1865.

(39) Jo, S.; Kim, T.; Im, W. Automated builder and database of protein/membrane complexes for molecular dynamics simulations. *PloS ONE.* **2007**, *2*, e880.

(40) Lomize, A. L.; Pogozheva, I. D.; Lomize, M. A.; Mosberg, H. I. Positioning of proteins in membranes: a computational approach. *Protein Sci.* **2006**, *15*, 1318–1333.

(41) Phillips, J. C.; Braun, R.; Wang, W.; Gumbart, J.; Tajkhorshid, E.; Villa, E.; Chipot, C.; Skeel, R. D.; Kalè, L.; Schulten, K. Scalable molecular dynamics with NAMD. *J. Comput. Chem.* **2005**, *26*, 1781–1802.

(42) Alex MacKerell. MacKerell laboratory home page. http://mackerell.umaryland.edu/MacKerell_Lab.html (accessed Jul 4, 2008).

(43) Humphrey, W.; Dalke, A.; Schulten, K. VMD: visual molecular dynamics. *J. Mol. Graph.* **1996**, *14*, 33–38.

(44) Theoretical and Computational Biophysics Group. http://www.ks.uiuc.edu/Research/vmd/plugins (accessed Jan 14, 2009).

(45) Cheatham Lab. Cheatham Lab WWW page. http://www.chpc.utah.edu/~cheatham/software.html (accessed Jan 21, 2009).

(46) Amadei, A.; Linssen, A. B.; Berendsen, H. J. Essential dynamics of proteins. *Proteins* **1993**, *17*, 412–425.

(47) Berk, H. Similarities between principal components of protein dynamics and random diffusion. *Phys. Rev.* **2000**, *62*, 8438–8448.
(48) Mongan, J. Interactive essential dynamics. *J. Comput.-Aided Mol. Des.* **2004**, *18*, 433–436.
(49) Trott, O.; Olson, A. J. *AutoDock Vina: improving the speed and accurancy of docking with a new scoring function, efficient optimization and multithreading*. http://vina.scripps.edu (accessed March 28, 2009).
(50) The Scripps Research Institute. MGL Tools. http://mgltools.scripps.edu (accessed March 28, 2009).
(51) Baker, R. W.; Chothia, C.; Pauling, P.; Weber, H. P. Molecular structures of hallucinogenic substances: lysergic acid diethylamide, psilocybin, and 2,4,5-trimethoxyamphetamine. *Mol. Pharmacol.* **1973**, *9*, 23–32.
(52) Cambridge Structural Database. http://www.ccdc.cam.ac.uk/products/csd/ (accessed March 28th, 2009).
(53) Tripos. http://www.tripos.com (accessed Jan 16, 2009).
(54) Kao, H. T.; Adham, N.; Olsen, M. A.; Weinshank, R. L.; Branchek, T. A.; Hartig, P. R. Site-directed mutagenesis of a single residue changes the binding properties of the serotonin 5-HT2 receptor from a human to a rat pharmacology. *FEBS Lett.* **1992**, *307*, 324–328.
(55) Roth, B. L.; Shoham, M.; Choudhary, M. S.; Khan, N. Identification of conserved residues essential for agonist binding and second messenger production at 5-Hydroxytriptamine$_{2A}$ receptors. *Mol. Pharmacol.* **1997**, *52*, 259–266.
(56) Roth, B. L.; Willins, D. L.; Kristiansen, K.; Kroeze, W. K. 5-Hydroxytryptamine2-family receptors (5-hydroxytryptamine2A, 5-hydroxytryptamine2B, 5-hydroxytryptamine2C): where structure meets function. *Pharmacol. Ther.* **1998**, *79*, 231–257.
(57) Shapiro, D. A.; Kristiansen, K.; Kroeze, W. K.; Roth, B. L. Differential modes of agonist binding to 5-hydroxytryptamine(2A) serotonin receptors revealed by mutation and molecular modeling of conserved residues in transmembrane region 5. *Mol. Pharmacol.* **2000**, *58*, 877–886.
(58) Kristiansen, K.; Kroeze, W. K.; Willins, D. L.; Gelber, E. I.; Savage, J. E.; Glennon, R. A.; Roth, B. L. A highly conserved aspartic acid (Asp-155) anchors the terminal amine moiety of tryptamines and is involved in membrane targeting of the 5-HT(2A) serotonin receptor but does not participate in activation via a "salt-bridge disruption" mechanism. *J. Pharmacol. Exp. Ther.* **2000**, *293*, 735–746.
(59) Ebersole, B. J.; Visiers, I.; Weinstein, H.; Sealfon, S. C. Molecular basis of partial agonism: orientation of indoleamine ligands in the binding pocket of the human serotonin 5HT2A receptor determines relative efficacy. *Mol. Pharmacol.* **2003**, *63*, 36–43.
(60) Braden, M. R.; Nichols, D. E. Assessment of the roles of serines 5.43(239) and 5.46(242) for binding and potency of agonist ligands at the human serotonin 5HT2A receptor. *Mol. Pharmacol.* **2007**, *72*, 1200–1209.

CI900067G